JACS
JOURNAL OF THE AMERICAN CHEMICAL SOCIETY
Article
pubs.acs.org/JACS

Bowl Inversion of Surface-Adsorbed Sumanene

Rached Jaafar,[†] Carlo A. Pignedoli,[†] Giovanni Bussi,[‡] Kamel Aït-Mansour,[†,§] Oliver Groening,[†] Toru Amaya,[∥] Toshikazu Hirao,[∥] Roman Fasel,[†,⊥] and Pascal Ruffieux*[,†]

[†]nanotech@surfaces Laboratory, Empa, Swiss Federal Laboratories for Materials Science and Technology, Überlandstrasse 129, 8600 Dübendorf, Switzerland

[‡]Scuola Internazionale Superiore di Studi Avanzati (SISSA), via Bonomea 265, 34136 Trieste, Italy

[§]Ecole Polytechnique Fédérale de Lausanne (EPFL), Institut de Physique de la Matière Condensée, Station 3, CH-1015 Lausanne, Switzerland

[∥]Department of Applied Chemistry, Graduate School of Engineering, Osaka University, Yamada-oka, Suita, Osaka 565-0871, Japan

[⊥]Department of Chemistry and Biochemistry, University of Bern, 3012 Bern, Switzerland

Supporting Information

ABSTRACT: Bowl-shaped π-conjugated compounds offer the possibility to study curvature-dependent host–guest interactions and chemical reactivity in ideal model systems. For surface-adsorbed π bowls, however, only conformations with the bowl opening pointing away from the surface have been observed so far. Here we show for sumanene on Ag(111) that both bowl-up and bowl-down conformations can be stabilized. Analysis of the molecular layer as a function of coverage reveals an unprecedented structural phase transition involving a bowl inversion of one-third of the molecules. On the basis of scanning tunneling microscopy (STM) and complementary atomistic simulations, we develop a model that describes the observed phase transition in terms of a subtle interplay between inversion-dependent adsorption energies and intermolecular interactions. In addition, we explore the coexisting bowl-up and -down conformations with respect to host–guest binding of methane. STM reveals a clear energetic preference for methane binding to the concave face of sumanene.

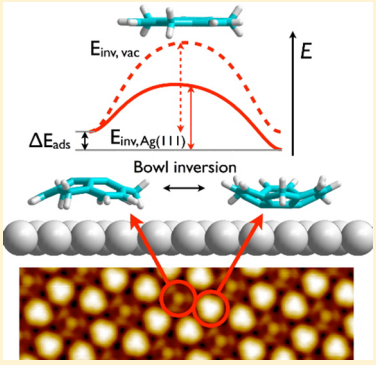

INTRODUCTION

Bowl-shaped π-conjugated compounds (commonly referred to as "open geodesic polyarenes", "buckybowls", or "π bowls"),[1−5] structurally related to fullerenes, represent a class of hydrocarbons with unique properties and potential for application as novel materials. The rich coordination chemistry of π bowls[5−8] allows for the formation of stable monolayers on metal surfaces,[9−11] which are important model systems for studying the electronic properties of organic/inorganic interfaces relevant in molecular electronics.[12−15] The curvature-induced rehybridization of the π orbitals has a pronounced effect on the chemical reactivity of π bowls[16,17] and is expected to increase the adsorption energy for guest molecules adsorbed within the bowl. This raises interest in π bowls as model systems for identifying high density and low pressure storage materials for weakly interacting energy carriers such as methane.[18,19] From the point of view of tunable host–guest interactions and controlled reactivity it would thus be highly desirable to control the inversion state of adsorbed π bowls (Figure 1). Bowl-to-bowl inversion is known as a characteristic behavior in solution, as reported, for example, for corannulene[20−22] and sumanene[23−25] (SUM) (Figure 1a). In the case of corannulene, the smallest 5-fold symmetric fullerene fragment, however, molecule–surface interactions on Cu surfaces clearly favor the inversion state where the bowl-opening is facing away from the surface.[9−11] For SUM, the smallest 3-fold symmetric fullerene fragment[4,26−28] (Figure 1a), studies of the bowl-to-bowl inversion revealed an inversion barrier of ∼0.9 eV in solution,[23] which is larger than that of the shallower corannulenes. Very recently, a related bidirectional concave to convex conformational switching has been reported for a surface-adsorbed porphyrin derivative.[29]

Here, we show for SUM that the inversion state of adsorbed molecules can be controlled via intermolecular interactions, thus making both inversion states accessible for investigation of their respective host–guest and reactivity properties. Specifically, we report on the molecular aggregation and conformation of SUM on Ag(111) as studied by means of scanning tunneling microscopy (STM) and complementary atomistic simulations. Analysis of the molecular layer as a function of coverage reveals an unprecedented structural phase transition involving a bowl inversion of one-third of the molecules. Atomistic simulations based on density functional theory (DFT) reveal that a subtle interplay between an inversion-dependent molecule–substrate binding energy and intermolecular interactions is at the heart of the observed transition.

Received: April 25, 2014
Published: September 2, 2014

   dx.doi.org/10.1021/ja504126z | J. Am. Chem. Soc. 2014, 136, 13666−13671

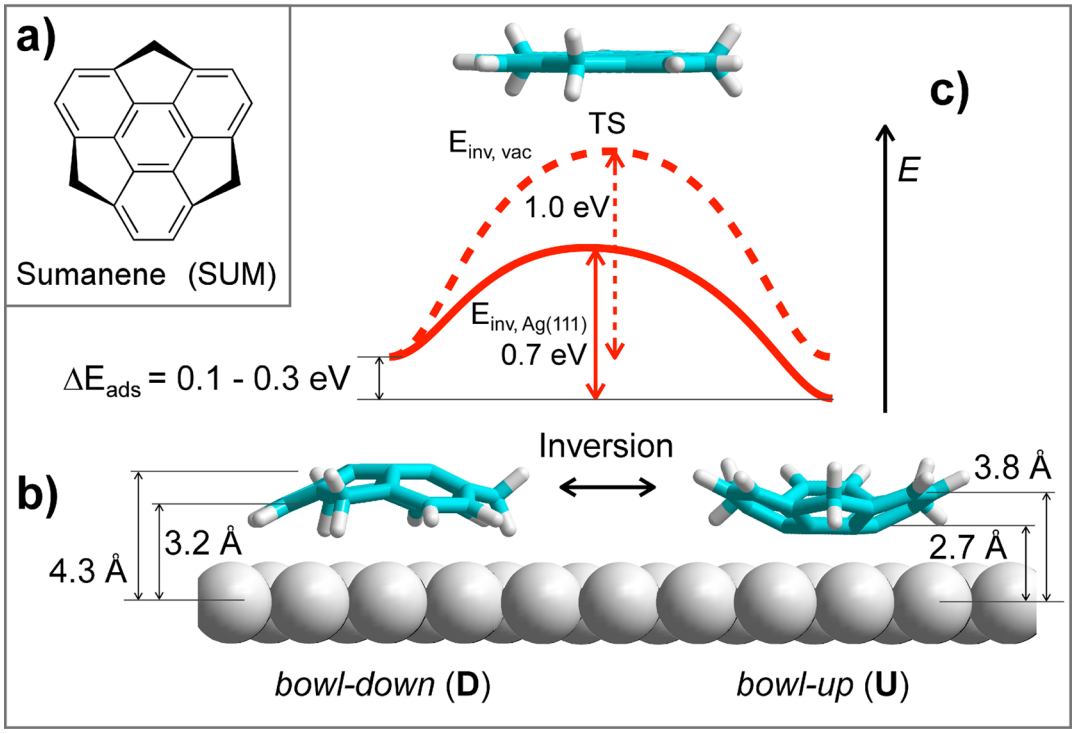

Figure 1. Bowl inversion of sumanene on Ag(111). (a) Molecular structure of sumanene (SUM). (b) Schematic view of the two possible inversion states of SUM on a metal surface. The computed adsorption heights of the hub and rim carbon atoms are indicated for both the bowl opening up (**U**) and down (**D**) configurations. (c) Inversion barriers from **D** to **U** via a planar transition state (TS) computed in vacuum (dashed line) and adsorbed on Ag(111) (full line).

RESULTS AND DISCUSSION

After deposition of 0.5 monolayer (ML) of SUM molecules on a clean Ag(111) surface under ultrahigh vacuum conditions, large-scale STM images show the presence of two distinct features (Figure 2a): randomly distributed small islands (**S** islands) composed of less than about 50 molecules, and large islands (**L** islands) extending over tens of nanometers. Figures 2b,c shows small-scale STM images of both island types, revealing that all molecules within **S** islands have the same apparent height, while two different height levels are observed for **L** islands. In both cases neighboring SUM molecules are spaced 1.0 nm apart, with nearest neighbor directions oriented along the ⟨1−21⟩ directions of the Ag substrate. Closer inspection of high resolution STM images such as the ones given in Figure 2b,c reveals that both island types are described by a hexagonal lattice with unit cell of side length 1.70 ± 0.04 nm containing three inequivalent molecules. This is compatible with a (6 × 6) superstructure with respect to the Ag(111) surface lattice and translates into a nearest neighbor SUM−SUM distance of 1.00 nm. For both types of islands, the three molecules within a unit cell take different azimuthal orientations (i.e., rotation with respect to an axis perpendicular to the surface). When sampling the occupied molecular states, such as in Figure 2b,c, the molecules' 3-fold symmetry is clearly apparent for both **S** and **L** islands. However, in **L** islands only two of the three molecules per unit cell show the same apparent height compared with those within **S** islands. The third molecule appears significantly higher and exhibits a characteristic ring-like contour at its center. While the relative height between the third and the two other molecules sensitively depends on the chosen sample bias (see the Supporting Information), the experimental images demonstrate that there are only two different molecular conformations present in the unit cell.

The detailed molecular conformations within **S** and **L** islands can be derived from a comparison of the experimental STM images to DFT-based simulations. Among the various configurations considered for simulation of filled-state STM images, we identify two that reproduce the main features of the experimental STM images from **S** and **L** islands, respectively (Figure 2b,c). Within **S** islands, all SUM molecules orient their bowl openings upward, i.e., away from the surface. We denote this adsorption configuration as bowl-up, and the corresponding SUM molecules as **U** for "bowl-up" (Figure 1b). We note that **U** molecules face the substrate surface with their central six-membered ring. For the **L** islands, we identify a configuration with only two **U** molecules and the third SUM bowl oriented upside down (bowl-down, **D**, Figure 1b). The corresponding STM simulations (Figure 2d,e) show excellent agreement with experiment and reveal that the three lobe features correspond to bowl-up (**U**) molecules, whereas the molecules imaged with higher apparent height are SUM molecules in bowl-down (**D**) configuration. We thus identify a significant structural difference between **S** and **L** islands: The unit cell of **S** islands consists of three bowl-up molecules (**3U**), but **L** islands are formed by two bowl-up and one bowl-down molecule (**2U1D**) per unit cell. The latter is a remarkable and unprecedented observation and raises questions about the origin of the corresponding phase transition, which we address in the following.

We start by examining the growth mode in some more detail (Figure 3). At a molecular coverage of 0.02 ML, a stochastic distribution of monomers and dimers is found on the surface (Figure 3a), with about 30% of the molecules forming dimers. Analysis of the island size distribution with increasing coverage

dx.doi.org/10.1021/ja504126z | J. Am. Chem. Soc. 2014, 136, 13666−13671

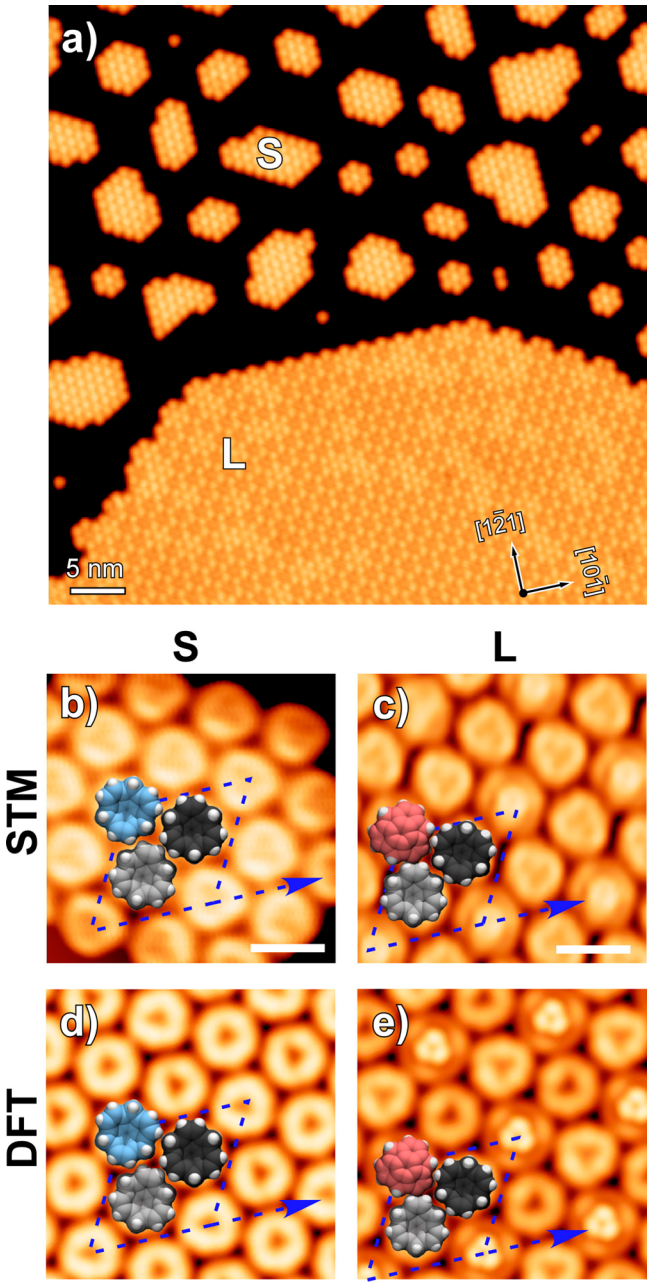

Figure 2. Coexistence of small (**S**) and large (**L**) islands of sumanene molecules on Ag(111). (a) Overview STM topography image revealing the coexistence of **L** and **S** islands at a coverage of 0.5 ML (U = 1.7 V, 0.05 nA, 5.3 K). Small scale experimental (b, c) and simulated (d, e) STM images of the occupied states (U = −0.5 V) in **S** islands (left) and **L** islands (right). Scale bars: 1 nm. Both island types illustrate a hexagonal lattice with unit cell (dashed blue) of side length 1.70 ± 0.04 nm and contain three inequivalent molecules (nearest neighbor spacings of 1.002 nm). **S** islands are found to consist entirely of bowl-up molecules (**3U** configuration), but **L** islands are formed by two bowl-up and one bowl-down molecule per unit cell (**2U1D**).

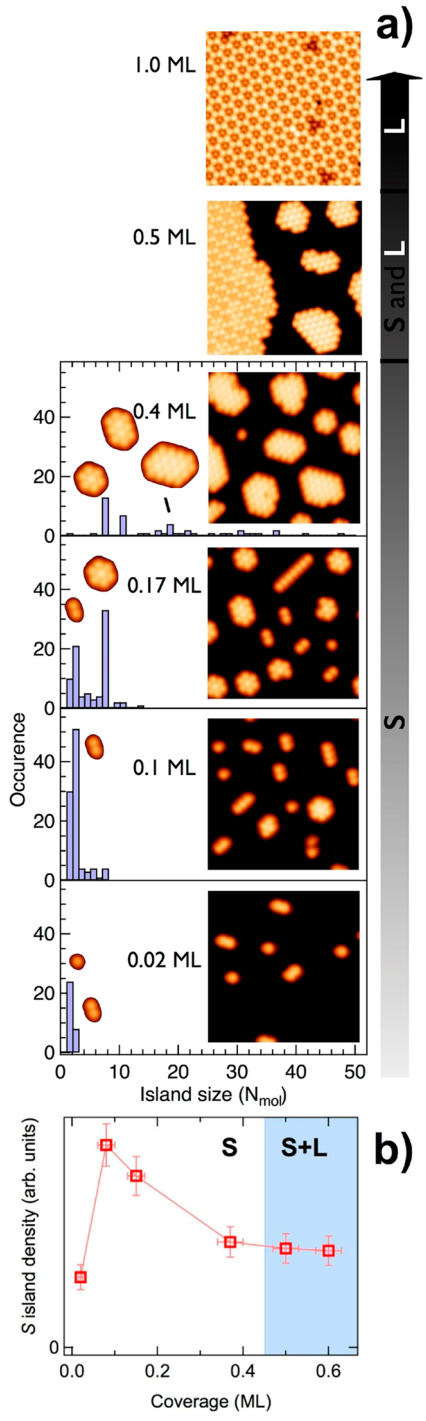

Figure 3. Coverage-dependent phase transition from small bowl-up islands to large domains with mixed bowl-up and bowl-down sumanenes. (a) STM images for increasing coverage of SUM on Ag(111) (20 × 20 nm^2, 5.6 K) and evaluation of the corresponding island size distribution for the small **S** islands consisting entirely of bowl-up (**U**) molecules. Insets show typical cluster geometries for the most frequent cluster sizes. (b) Island density in **S** regions as a function of molecular coverage.

reveals that distinct "closed-shell" configurations are preferred, indicating that molecules are highly mobile at deposition temperature. The fact that for coverages up to 0.1 ML both the number of islands (island density) and the island size grow simultaneously indicates that the island size and their distribution on the substrate terraces is given by a subtle interplay between intermolecular interactions and a repulsive interaction between islands. Upon further increase of the coverage to 0.4 ML, the island size further increases while their density decreases continuously (Figure 3b). Then a dramatic change of the growth mode occurs at about 0.45 ML coverage, when the **S** islands have reached a maximum island size of about 50 molecules (Figure 3). Instead of further increasing **S**

dx.doi.org/10.1021/ja504126z | J. Am. Chem. Soc. 2014, 136, 13666−13671

island size or density, molecules exceeding the local 0.45 ML coverage in the **S** domains are accommodated in a concomitantly appearing new domain containing large **L** islands. For a SUM coverage above ~0.5 ML the number of the **L** islands rapidly increases while the area occupied by the **S** island domain that maintains the local 0.45 ML coverage (Figure 3b) is decreasing until the **L** islands cover the entire surface area. We note that the critical coverage of 0.45 ML at which the transition between pure **S** domains and mixed **S** and **L** domains occurs does not depend on whether the sample is rapidly cooled in the cryostat precooled to 5 K or more gently in the cryostat precooled to 77 K. Accordingly, the observed ratio between **S** and **L** domains is not affected by kinetics but rather is the thermodynamically preferred molecular structure.

The transition from **S** islands with three **U** molecules per unit cell (**3U** configuration) to **L** islands with two **U** molecules and one **D** molecule per unit cell (**2U1D** configuration) involves a bowl inversion of one-third of the SUM molecules. To understand the origin of this transition, we studied the molecule−molecule and molecule−substrate interactions by means of DFT calculations including empirical van der Waals corrections.[30] We performed calculations both in vacuum and with inclusion of the Ag(111) substrate for single molecules as well as for extended two-dimensional (2D) islands (see Supporting Information for details).

First, we emphasize that the transition from the **3U** to the **2U1D** configuration cannot be explained by a simple "roll over" of one-third of the SUM molecules; such rotational transition from **U** to **D** involves an energy barrier of the order of the adsorption energy, which we calculate within DFT to be 1.5 eV for a **U** molecule facing the substrate with its central six-membered ring. We find, however, that the surface interaction significantly lowers the barrier to bowl inversion from 1 eV for SUM in vacuum to 0.7 eV for a SUM molecule adsorbed on Ag(111) (Figure 1c, see Supporting Information for computational details). This inversion barrier is easily overcome at room temperature: Within an Arrhenius picture and an estimated attempt frequency of 1×10^{13} s^{-1}, a barrier of 0.7 eV translates into a bowl inversion rate of about 10^3 s^{-1} or a half-life of 6×10^{-3} s. But what stabilizes one inversion state rather than the other one? For isolated SUM molecules adsorbed on Ag(111), our DFT calculations show that the bowl-up (**U**) adsorption geometry is energetically favored by about 0.1 eV over the bowl-down (**D**) configuration. This naturally explains the observed **U** configuration of isolated adsorbed SUM molecules.

Next we consider the other extreme, i.e., extended 2D islands. We find that the **2U1D** configuration (**L** islands) is favored by 0.1 eV per molecule over the **3U** one (**S** islands), again in agreement with experimental observations. This suggests that on Ag(111) **U** molecules are more stable unless interactions within the adsorbed layer induce the transition to **2U1D** islands. Such transition between **3U** and **2U1D** configurations is thus the result of a subtle interplay between (i) a difference in adsorption energy for **U** and **D** molecules (0.1−0.3 eV; see Supporting Information), (ii) molecular interactions **U**−**D** and **U**−**U**, and (iii) possible longer range interactions.

To address point ii above, we show the gas phase molecule−molecule pair potential as derived from DFT calculations in Figure 4a. The **U**−**U** (blue line) and **U**−**D** (red line) interaction energy is plotted as a function of normalized intermolecular distance d/d_0 where d_0 = 1.002 nm is the nearest neighbor distance for a SUM island with Ag(111)-(6 × 6) superstructure as determined from experiment. The location of the minimum of the red line in Figure 4a reveals that the **2U1D** lattice is almost perfectly commensurate (d/d_0 = 1.007) with the substrate while the shifted position of the blue curve shows that the **3U** configuration prefers a significantly expanded unit cell (d/d_0 = 1.051). On the basis of this evidence, we discuss a simple model to explain the coverage-dependent transition from **S** islands with **3U** configuration of molecules to **L** islands with **2U1D** configuration in terms of mismatch energy accumulated with increasing **3U** island size. Figure 4a shows that inversion of a SUM molecule from **U** to **D** leads, in terms of intermolecular interactions, to an energy gain of ~0.24 eV. On the other hand, the inversion from **U** to **D** (inside a island)

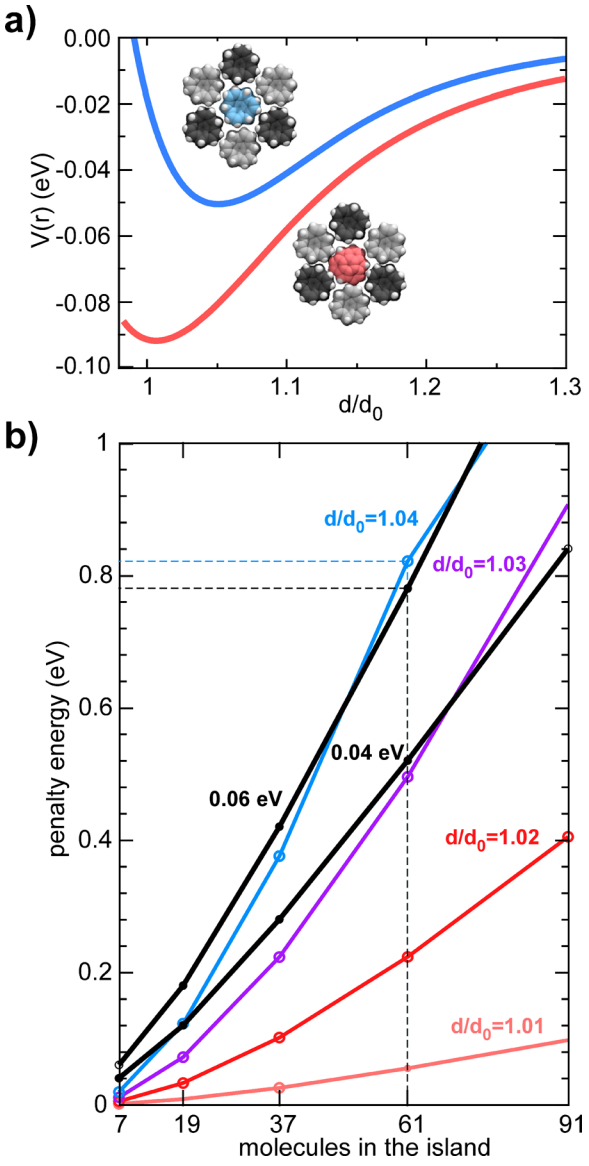

Figure 4. Mechanism of the phase transition involving bowl inversion of every third SUM molecule. (a) Molecular pair potential as derived from DFT calculations for **U**−**U** (blue line) and **U**−**D** (red line) pairs (substrate not considered). (b) Comparison of the penalty energies arising from strain in **3U** islands (colored lines) and from **U**/**D** inversion into **2U1D** ones (black lines) as a function of island size expressed as molecules per island. The colored lines correspond to strain of 1% to 4% as labeled. The two black lines correspond to 0.04 and 0.06 eV total energy gain per molecule, respectively.

dx.doi.org/10.1021/ja504126z | J. Am. Chem. Soc. 2014, 136, 13666−13671

entails a decrease in adsorption energy of 0.1−0.3 eV (depending on computational models; see Supporting Information). If only nearest neighbor interactions are considered, islands are thus expected to be stable either in the **3U** geometry or in the **2U1D** configuration depending on the exact values of the energy gain/loss discussed above.

We thus also need to address point iii above, i.e., possible longer range interactions. Note that **S** islands with **3U** configuration are only stable up to a maximum island size of about 50 molecules, which indicates that strain accumulated with increasing island size might provide the missing ingredient to drive the phase transition from **3U** to **2U1D**. Indeed, Figure 4a shows that **S** (**3U**) islands have an equilibrium lattice constant d_{3U} larger than d_0 and are thus significantly compressed on Ag(111) where they are observed to take the d_0 = 1.00 nm lattice constant imposed by (6 × 6) substrate commensurability. To estimate the impact of such strain, we compute the mismatch penalty energy (strain energy) accumulated in **3U** islands of increasing size (number of molecules varying from 7 to 91) for equilibrium lattice constants d_{3U} that are 1%, 2%, 3%, and 4% larger than the commensurate d_0 value of 1.00 nm (for details, see Supporting Information). In Figure 4b, we compare the corresponding mismatch penalty energies to the interaction energy penalty arising from **U** to **D** bowl inversion or more precisely from transforming a **3U** island into a **2U1D** island of corresponding size that is perfectly commensurate to the substrate (d_{2U1D} = d_0). The latter consists of the two contributions discussed above, namely the loss in adsorption energy upon **U** to **D** bowl inversion and the corresponding gain in molecule−molecule interaction in going from a **3U** to a **2U1D** configuration. The black lines in Figure 4b correspond to 0.04 and 0.06 eV total energy gain per molecule in the **2U1D** configuration. The lower one crosses the dark blue line (lattice compression of 3%) at an islands size of 61 molecules. For 3% of strain and 0.04 eV interaction energy penalty upon **U**−**D** inversion, **3U** islands are thus initially favored, but the accumulated strain drives the islands into the **2U1D** configuration for islands larger than 61 molecules. This simple model thus provides a mechanism that rationalizes the observed transition between **S** islands with **3U** configuration of SUM molecules into **L** islands with **2U1D** configuration beyond a critical island size (see Supporting Information for additional details).

While this simple model catches the main features of the experimentally observed phase transition, and in particular the accompanying bowl inversion, it certainly does not describe all details of the observed growth mode. We have thus also explored more elaborate models to gain further insight into the intriguing coverage-dependent phase transition of SUM on Ag(111) and the associated bowl inversion. In the Supporting Information we discuss a model based on rigid lattice Monte Carlo simulations, where in addition to first neighbor interactions also long-range repulsion is included. Interestingly, this alternative model, that does not rely on strain accumulation but on long-range repulsive interactions, also reproduces the experimentally observed behavior: At low coverages, small islands of **U** molecules are obtained (**S** islands), while at higher coverages, **L** islands with **2U1D** configuration are energetically more favorable. We conclude that three key ingredients drive the observed phase transition/bowl inversion: (i) a higher adsorption energy for bowl-up (**U**) than for bowl-down (**D**) molecules, (ii) a higher pair attraction energy for **U**−**D** than for **D**−**D** and **U**−**U** pairs, and (iii) either strain accumulation in islands of **U** molecules due to lattice mismatch with the underlying Ag(111) surface or a long-range repulsive interaction that is stronger for **U**−**U** than for **U**−**D** pairs (e.g., from different amounts of charge transfer).

Finally, we explore the concave as well as convex faces of SUM with respect to host−guest interactions by adsorption of methane on an intermediate coverage SUM/Ag(111) sample with coexisting **S** and **L** islands (Figure 5). For methane dosage

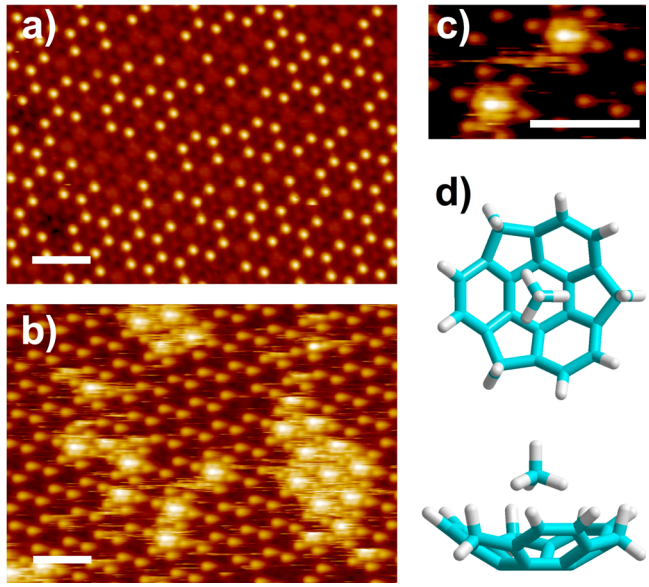

Figure 5. Methane adsorption on SUM. (a) STM image of a **2U1D** island after dosing ∼0.4 L of methane at 12 K on SUM adsorbed on Ag(111) (−0.5 V, 12 pA, 5 K). Methane guests are imaged as single bright spots and are exclusively found at positions corresponding to bowl-up (**U**) hosts. (b) STM image of a **2U1D** island for ∼1.2 L of methane. Methane adsorbates that cannot be accommodated by **U** molecules assemble to heptamer clusters located around bowl-down (**D**) molecules (−1.5 V, 5 pA, 5 K). (c) Small-scale STM image revealing methane guests in **U** SUM hosts as well as two methane heptamer clusters centered on **D** SUM molecules. (d) Structural model of the observed SUM-methane host−guest complex (top and side views). Scale bars: 3 nm.

at ∼30 K, we find adsorption on both types of islands. In **S** islands (**U** molecules) all SUMs can accommodate a methane guest (not shown). In **L** islands, however, only **U** molecules (bowl-up configuration) host methane (Figure 5a), whereas **D** molecules do not bind methane guests. For the weakly interacting methane, this evidences a clear adsorption preference for the concave over the convex side of the π bowl. Only at higher methane dosage and after full occupation of all available **U** host sites are adsorption sites in the vicinity of **D** SUMs getting decorated (Figure 5b). From STM images, we identify close-packed methane heptamer clusters centered on **D** molecules in addition to the singly occupied **U** SUMs. Clusters with less than seven methane molecules cannot be stably imaged, indicating that individual methane molecules are not stably adsorbed on or near **D** (bowl opening down) molecules. The observed clear preference for methane adsorption on **U** molecules is corroborated by computed methane−SUM binding energies that amount to 0.12 eV on the concave side (**U**) but only to 0.06 eV on the convex (**D**) side of SUM.

In conclusion, we have identified and characterized an intriguing coverage-dependent phase transition involving bowl

dx.doi.org/10.1021/ja504126z | J. Am. Chem. Soc. 2014, 136, 13666−13671

inversion for sumanene on a Ag(111) surface. For low sumanene coverage, islands with all bowl openings pointing away from the surface are observed. At higher coverage, bowl inversion of one-third of the molecules is activated by accumulated strain and stabilized by enhanced intermolecular interaction. At monolayer coverage, the sumanene on Ag(111) system thus provides the unprecedented case of a π-bowl layer with concave as well as convex faces pointing away from the surface. This mixed inversion state layer provides an ideal template for investigations of site- and inversion state-specific host−guest interactions and offers the opportunity to explore the curvature-dependent reactivity against physically or chemically interacting adsorbates. As a first step along these lines, we have demonstrated the selective adsorption of methane on the concave side of sumanene.

EXPERIMENTAL AND COMPUTATIONAL DETAILS

STM experiments were performed with a commercial low temperature STM (Omicron) operated in ultrahigh vacuum. Ag(111) single crystal surfaces were prepared by repeated cycles of sputtering with Ar^+ ions at $\sim 4 \times 10^{-6}$ mbar and annealing to 700 K for 15 min at pressures below 5×10^{-10} mbar. LEED and STM were used to check the quality of the surface before deposition of molecules. SUM molecules were deposited by molecular beam epitaxy at 410 K from a homemade Knudsen-cell-type evaporator onto the Ag(111) surface kept at room temperature (deposition rate of about 1 Å/min as monitored with a quartz crystal microbalance). STM measurements were taken in constant-current mode for as-deposited samples cooled to the indicated temperature. Indicated tunneling bias voltages are given with respect to the sample, and STM data were analyzed with WSXM software.[31] DFT simulations of adsorption energies, equilibrium geometries, and inversion barriers were performed in the mixed plane wave Gaussian framework implemented in the cp2k code[32] with inclusion of semiempirical van der Waals corrections.[30] STM simulations were performed within the Tersoff Haman approximation.[33] Inversion barriers were computed using the NEB method with climbing image[34] (see Supporting Information for further details).

ASSOCIATED CONTENT

Supporting Information

Details for DFT calculations, Monte Carlo simulations, and additional STM images. This material is available free of charge via the Internet at http://pubs.acs.org.

AUTHOR INFORMATION

Corresponding Author

pascal.ruffieux@empa.ch

Notes

The authors declare no competing financial interest.

ACKNOWLEDGMENTS

We acknowledge the Swiss National Science Foundation (SNF) for financial support and the Swiss National Supercomputing Centre (CSCS) for computational resources.

REFERENCES

(1) Wu, Y.-T.; Siegel, J. S. *Chem. Rev.* **2006**, *106*, 4843−4867.
(2) Tsefrikas, V. M.; Scott, L. T. *Chem. Rev.* **2006**, *106*, 4868−4884.
(3) Higashibayashi, S.; Sakurai, H. *Chem. Lett.* **2011**, *40*, 122−128.
(4) Amaya, T.; Hirao, T. *Chem. Commun.* **2011**, *47*, 10524−10535.
(5) *Fragments of fullerenes and carbon nanotubes: designed synthesis, unusual reactions, and coordination chemistry*; Scott, L. T.; Petrukhina, M. A., Eds.; John Wiley & Sons: Hoboken, NJ, 2011.
(6) Petrukhina, M. A.; Scott, L. T. *Dalton Trans.* **2005**, 2969−2975.
(7) Filatov, A. S.; Petrukhina, M. A. *Coord. Chem. Rev.* **2010**, *254*, 2234−2246.
(8) Petrukhina, M. A. *Angew. Chem., Int. Ed* **2008**, *47*, 1550−1552.
(9) Parschau, M.; Fasel, R.; Ernst, K.; Gröning, O.; Brandenberger, L.; Schillinger, R.; Greber, T.; Seitsonen, A.; Wu, Y.; Siegel, J. *Angew. Chem., Int. Ed.* **2007**, *46*, 8258−8261.
(10) Xiao, W.; Passerone, D.; Ruffieux, P.; Aït-Mansour, K.; Gröning, O.; Tosatti, E.; Siegel, J. S.; Fasel, R. *J. Am. Chem. Soc.* **2008**, *130*, 4767−4771.
(11) Bauert, T.; Merz, L.; Bandera, D.; Parschau, M.; Siegel, J. S.; Ernst, K.-H. *J. Am. Chem. Soc.* **2009**, *131*, 3460−3461.
(12) Joachim, C.; Gimzewski, J.; Aviram, A. *Nature* **2000**, *408*, 541−548.
(13) Barth, J. V.; Costantini, G.; Kern, K. *Nature* **2005**, *437*, 671−679.
(14) Barth, J. V. *Annu. Rev. Phys. Chem.* **2007**, *58*, 375−407.
(15) Cuevas, J. C.; Scheer, E. *Molecular Electronics: An Introduction to Theory and Experiment*; World Scientific: Hackensack, NJ, 2010; Vol. *1*.
(16) Ruffieux, P.; Gröning, O.; Bielmann, M.; Mauron, P.; Schlapbach, L.; Gröning, P. *Phys. Rev. B* **2002**, *66*, 245416.
(17) Chen, Z.; Thiel, W.; Hirsch, A. *ChemPhysChem* **2003**, *4*, 93−97.
(18) Makal, T. A.; Li, J.-R.; Lu, W.; Zhou, H.-C. *Chem. Soc. Rev.* **2012**, *41*, 7761−7779.
(19) Alcaniz-Monge, J.; Lozano-Castello, D.; Cazorla-Amoros, D.; Linares-Solano, A. *Microporous Mesoporous Mater.* **2009**, *124*, 110−116.
(20) Scott, L. T.; Hashemi, M. M.; Bratcher, M. S. *J. Am. Chem. Soc.* **1992**, *114*, 1920−1921.
(21) Sygula, A.; Abdourazak, A. H.; Rabideau, P. W. *J. Am. Chem. Soc.* **1996**, *118*, 339−343.
(22) Seiders, T. J.; Baldridge, K. K.; Grube, G. H.; Siegel, J. S. *J. Am. Chem. Soc.* **2001**, *123*, 517−525.
(23) Amaya, T.; Sakane, H.; Muneishi, T.; Hirao, T. *Chem. Commun.* **2008**, 765−767.
(24) Amaya, T.; Sakane, H.; Nakata, T.; Hirao, T. *Pure Appl. Chem.* **2010**, *82*, 969−978.
(25) Amaya, T.; Hirao, T. *Pure Appl. Chem.* **2012**, *84*, 1089−1100.
(26) Sakurai, H.; Daiko, T.; Hirao, T. *Science* **2003**, *301*, 1878.
(27) Sakurai, H.; Daiko, T.; Sakane, H.; Amaya, T.; Hirao, T. *J. Am. Chem. Soc.* **2005**, *127*, 11580−11581.
(28) Amaya, T.; Sakane, H.; Hirao, T. *Angew. Chem., Int. Ed.* **2007**, *46*, 8376−8379.
(29) Ditze, S.; Stark, M.; Buchner, F.; Aichert, A.; Jux, N.; Luckas, N.; Görling, A.; Hieringer, W.; Hornegger, J.; Steinrück, H.-P.; Marbach, H. *J. Am. Chem. Soc.* **2014**, *136*, 1609−1616.
(30) Grimme, S.; Antony, J.; Ehrlich, S.; Krieg, H. *J. Chem. Phys.* **2010**, *132*, 154104.
(31) Horcas, I.; Fernandez, R.; Gomez-Rodriguez, J. M.; Colchero, J.; Gomez-Herrero, J.; Baro, A. M. *Rev. Sci. Instrum.* **2007**, *78*, 013705.
(32) VandeVondele, J.; Krack, M.; Mohamed, F.; Parrinello, M.; Chassaing, T.; Hutter, J. *Comput. Phys. Commun.* **2005**, *167*, 103−128.
(33) Tersoff, J.; Hamann, D. R. *Phys. Rev. Lett.* **1983**, *50*, 1998−2001.
(34) Henkelman, G.; Uberuaga, B. P.; Jónsson, H. *J. Chem. Phys.* **2000**, *113*, 9901.